

The Magnetic Susceptibility of Strongly Interacting Matter across Deconfinement

Claudio Bonati,^{*} Massimo D'Elia,[†] and Marco Mariti[‡]
Dipartimento di Fisica dell'Università di Pisa and INFN - Sezione di Pisa,
Largo Pontecorvo 3, I-56127 Pisa, Italy

Francesco Negro[§]
Dipartimento di Fisica dell'Università di Genova and INFN - Sezione di Genova,
Via Dodecaneso 33, I-16146 Genova, Italy

Francesco Sanfilippo[¶]
Laboratoire de Physique Théorique (Bat. 210) Université Paris SUD, F-91405 Orsay-Cedex, France
 (Dated: January 27, 2023)

We propose a method to determine the total magnetic susceptibility of strongly interacting matter by lattice QCD simulations, and present first numerical results for the theory with two light flavors, which suggest a very weak magnetic activity in the confined phase and the emergence of strong paramagnetism in the deconfined, Quark-Gluon Plasma phase.

PACS numbers: 12.38.Aw, 11.15.Ha, 12.38.Gc, 12.38.Mh

I. INTRODUCTION

Understanding the properties of strongly interacting matter in presence of strong magnetic backgrounds is a problem of the utmost phenomenological importance. The physics of the early Universe evolution [1, 2], of non-central heavy ion collisions [3–6] and of compact astrophysical objects, like magnetars [7], is strictly related to that, involving fields going from 10^{10} Tesla in magnetars up to 10^{15-16} Tesla (i.e. $|e|B \sim 1 \text{ GeV}^2$) in heavy ion collisions and in the early Universe. The problem is also relevant to a better comprehension of the non-perturbative properties of QCD and of the Standard Model in general. That justifies the recent theoretical efforts on the subject (see, e.g., Ref. [8]).

Any material is characterized by the way it reacts to electromagnetic external sources. For strongly interacting matter, such as that present in the Early Universe and in the core of compact astrophysical objects, or that created in heavy ion collisions, the same questions as for any other medium can be posed. Does it react linearly to magnetic backgrounds, at least for small fields, and is it a paramagnet or a diamagnet? What is the behavior of the magnetic susceptibility, χ , as a function of the temperature T and/or chemical potentials?

Despite the clear-cut nature of such questions, a definite answer is still missing. Strong interactions in external fields can be conveniently explored by lattice QCD simulations, however various investigations have focussed till now only on partial aspects, like the magnetic prop-

erties of the spin component [9, 10] and of the QCD vacuum [11]. Most technical difficulties are related to the fact that in a lattice setup, which usually adopts toroidal geometries, the magnetic background is quantized.

In the following we propose a new method to overcome such difficulties, and we present a first investigation for QCD with 2 light flavors in the standard rooted staggered formulation, performed at various values of the lattice spacing a and of the quark masses. Results show that χ is very small (vanishing within present errors) in the confined phase, while it steeply rises above the transition, i.e. the Quark-Gluon Plasma is a paramagnetic medium.

II. THE METHOD

The magnetic properties of a homogeneous medium at thermal equilibrium can be inferred from the change of its free energy density, $f = F/V$, in terms of an applied constant and uniform field:

$$\Delta f(B, T) = -\frac{T}{V} \log \left(\frac{Z(B, T, V)}{Z(0, T, V)} \right) \quad (1)$$

where $Z = \exp(-F/T)$ is the partition function of the system, B is the magnetic field modulus and V is the spatial volume. One usually deals directly with free energy derivatives, like the magnetization, which can be rewritten in terms of thermal expectation values and are extracted more easily than free energy differences, whose computation is notoriously difficult.

However, in lattice simulations some difficulties emerge, related to the need for a finite spatial volume. The best way to accomplish that, while minimizing finite size effects and keeping a homogeneous background field, is to work on a compact manifold without boundaries: a 3D torus (cubic lattice with periodic boundary conditions) is a typical standard choice. It is well known that

^{*}Electronic address: bonati@df.unipi.it

[†]Electronic address: delia@df.unipi.it

[‡]Electronic address: mariti@df.unipi.it

[§]Electronic address: fnegro@ge.infn.it

[¶]Electronic address: francesco.sanfilippo@th.u-psud.fr

such choice leads to ambiguities in presence of charged particles moving over the manifold, unless the total flux of the magnetic field, across a section of the manifold orthogonal to it, is quantized in units of $2\pi/q$, where q is the elementary electric particle charge. The same argument leads to Dirac quantization of the magnetic monopole charge, when considering a spherical surface around it. In the case of the 3D torus, assuming $\mathbf{B} = B \hat{z}$ and considering that for quarks $q = |e|/3$, one has [12–15]

$$|e|B = \frac{6\pi b}{l_x l_y} \quad (2)$$

where b is an integer and l_x, l_y are the torus extensions in the x, y directions.

Since the field is quantized, taking derivatives with respect to it is not a well defined operation: this is the problem that prevented previous studies from a full determination of the magnetic properties of QCD [10, 11]. However, one can still go back to Eq. (1) and consider finite free energy differences: this is our strategy. In order to better illustrate it, let us recall some more details regarding the magnetic field on the lattice torus.

Electromagnetic fields enter the QCD lagrangian through the covariant derivative of quarks, $D_\mu = \partial_\mu + i g A_\mu^a T^a + i q A_\mu$, where A_μ is the electromagnetic gauge potential and q is the quark electric charge. On the lattice, that corresponds to adding proper $U(1)$ phases $u_\mu(n)$ to the $SU(3)$ parallel transports entering the discretized Dirac operator, $U_\mu(n) \rightarrow u_\mu(n) U_\mu(n)$, where n is a lattice site. A magnetic field $\mathbf{B} = B \hat{z}$ can be realized, for instance, by a potential $A_y = Bx$ and $A_\mu = 0$ for $\mu \neq y$. In presence of periodic boundary conditions, B must be quantized as in Eq. (2) and proper b.c. must be chosen for fermions, to preserve gauge invariance [15]. The corresponding $U(1)$ links are

$$\begin{aligned} u_y^{(q)}(n) &= e^{i a^2 q B n_x} = e^{i 2\pi b n_x / (L_x L_y)} \\ u_x^{(q)}(n)|_{n_x=L_x} &= e^{-i a^2 q L_x B n_y} = e^{-i 2\pi b n_y / L_y} \end{aligned} \quad (3)$$

and $u_\nu(n) = 1$ otherwise, where $n_\mu \in \{1, \dots, L_\mu\}$ and L_μ is the number of lattice sites in the μ direction.

With this choice, a constant magnetic flux $a^2 B$ goes through all plaquettes in the xy plane, apart from a “singular” plaquette located at $n_x = L_x$ and $n_y = L_y$, which is pierced by a flux $(1 - L_x L_y) a^2 B$, leading to a vanishing total flux through the xy torus, as expected for a closed surface. In the continuum limit, that corresponds to a uniform magnetic field plus a Dirac string piercing the torus in one point: like for Dirac monopoles, the string carries all the flux away. However, if B is quantized as in Eq. (2), the string becomes invisible to all particles carrying electric charges multiple of q , and the phase of the singular plaquette becomes equivalent, modulo 2π , to that of all other plaquettes, i.e. the field is uniform.

Let us now face the problem of computing finite free energy differences, $f(B_2) - f(B_1) = f(b_2) - f(b_1)$ where b_1 and b_2 are integers. Several methods are known to

determine such differences in an efficient way (see, e.g., Ref. [16]): the general idea is to divide the difference into a sum of smaller, easily computable differences. We will consider infinitesimal differences and rewrite

$$f(b_2) - f(b_1) = \int_{b_1}^{b_2} \frac{\partial f(b)}{\partial b} db, \quad (4)$$

the idea being to determine the integral after computing the integrand on a grid of points, fine enough to keep systematic errors under control.

Let us clarify the meaning of $\partial f / \partial b$ for generic real values of b , corresponding to a uniform magnetic field plus a visible Dirac string. While this is not the physical situation we are interested in, it still represents a legitimate theory, interpolating between integer values of b . In practice, we are extending a function, originally defined on integers, to the real axis, and then we are integrating its derivative between integer values to recover the original function: as long as the extension is analytic, which is always the case on a finite lattice, the operation is well defined (see Appendix A for an explicit check).

Let us stress that the quantity $\partial f / \partial b$, whose explicit form is given later on, has nothing to do with the magnetization of the system: in fact, a large contribution to it comes from the string itself, as it will be evident from its oscillating behavior. Moreover, the free energy has a local minimum when the string becomes invisible, hence $\partial f / \partial b$ vanishes when b is an integer.

A. Renormalization

The procedure described above gives access to $\Delta f(B, T)$, defined in Eq. (1), however we have to take care of divergent contributions. Indeed, B -dependent divergences do not cancel when taking the difference Δf , and must be properly subtracted, with possible ambiguities related to the definition of the vacuum energy in presence of a magnetic field. For $T = 0$, the prescription of Ref. [11] is to subtract all terms quadratic in B , so that, by definition, the magnetic properties of the QCD vacuum are of higher order in B .

In the following, we are not interested in the magnetic properties of vacuum, but only in those of the strongly interacting thermal medium, which may be probed experimentally. Therefore, our prescription is to compute the following quantity:

$$\Delta f_R(B, T) = \Delta f(B, T) - \Delta f(B, 0) \quad (5)$$

which is properly renormalized, since all vacuum (zero T) contributions have been subtracted and no further divergences, depending both on B and on T , appear (see, e.g., the discussion in Refs. [11, 17]). Clearly, divergences are really removed only if the contributions to Eq. (5) are evaluated at a fixed value of the lattice spacing. The small field behavior of Δf_R will give access to the magnetic susceptibility of the medium.

L_s	L_t	β	am	$a[\text{fm}]$	$m_\pi[\text{MeV}]$	$T[\text{MeV}]$	$\tilde{\chi} \times 10^3$
20	4	5.4075	0.00334	0.188	195	262	3.76(41)
16	4	5.4342	0.00584	0.17	275	290	4.06(27)
16	6	5.4342	0.00584	0.17	275	193	1.39(30)
16	8	5.4342	0.00584	0.17	275	145	0.45(46)
24	4	5.527	0.0146	0.141	480	349	5.32(40)
24	6	5.527	0.0146	0.141	480	233	2.82(33)
24	8	5.527	0.0146	0.141	480	175	0.97(41)
24	10	5.527	0.0146	0.141	480	140	0.29(40)
16	4	5.453	0.02627	0.188	480	262	3.06(19)
16	6	5.453	0.02627	0.188	480	175	0.42(22)
16	8	5.453	0.02627	0.188	480	131	0.10(22)
16	4	5.3945	0.0495	0.24	480	205	1.02(14)
16	8	5.3945	0.0495	0.24	480	103	0.03(17)

TABLE I: Lattice parameters and results for $\tilde{\chi}$.

B. Effects of QED quenching

In this work, electromagnetic degrees of freedom are treated as external sources, i.e. their dynamics is quenched. Let us discuss the effects of that.

When studying magnetism in matter, it is customary to introduce three vectors: the true magnetic field \mathbf{B} , the magnetization per volume unit \mathbf{M} and the auxiliary vector \mathbf{H} , defined by $\mathbf{B} = \mu_0(\mathbf{H} + \mathbf{M})$ (using SI units), i.e. the field generated by external currents only. For small fields and for a linear, homogeneous and isotropic medium, \mathbf{M} is proportional to \mathbf{B} . The proportionality is expressed through the magnetic susceptibility $\tilde{\chi}$, defined by $\mathbf{M} = \tilde{\chi}\mathbf{B}/\mu_0$, or, as more usual, through the magnetic permittivity μ and the susceptibility χ , defined by

$$\mathbf{M} = \chi\mathbf{H}; \quad \mathbf{B} = \mu\mathbf{H}; \quad \mu = \mu_0(1 + \chi), \quad (6)$$

where the relation $\chi = \tilde{\chi}/(1 - \tilde{\chi})$ holds.

The change in the free energy density is usually written in the form $\Delta f = \int \mathbf{H} \cdot d\mathbf{B}$ (see, e.g., Ref. [18] §31). However, in Δf_R the self-energy of the magnetic field is subtracted, hence the proper expression is:

$$\Delta f_R = - \int \mathbf{M} \cdot d\mathbf{B}. \quad (7)$$

The magnetic field \mathbf{B} entering Eq. (7) should be the total field acting on the medium, i.e. the external field plus the back-reaction from the medium itself. However, if QED degrees of freedom are quenched, the back-reaction is absent and the external and the total field coincide. Taking into account that $\mathbf{M} = \tilde{\chi}\mathbf{B}$, we finally get, in the limit of small fields,

$$\Delta f_R = - \frac{\tilde{\chi}}{\mu_0} \int \mathbf{B} \cdot d\mathbf{B} = - \frac{\tilde{\chi}}{2\mu_0} \mathbf{B}^2. \quad (8)$$

Hence, because QED quenching, we access directly $\tilde{\chi}$.

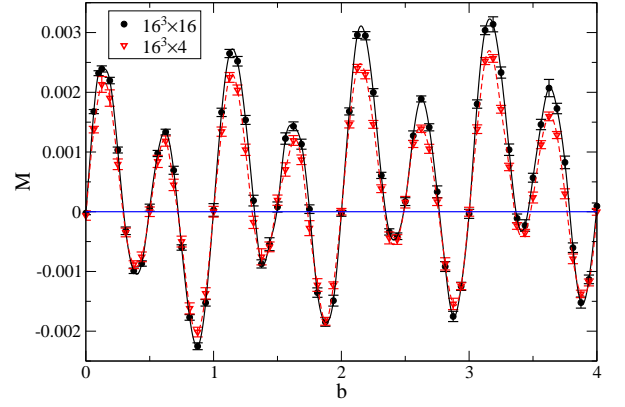


FIG. 1: M computed on 16^4 and $16^3 \times 4$ lattices, with $a \approx 0.188$ fm and $m_\pi \approx 480$ MeV. The continuous and dashed lines are third order spline interpolations.

III. NUMERICAL RESULTS

As a first application of our method, we consider $N_f = 2$ QCD with fermions discretized with the standard rooted staggered formulation, in which each quark is described by the fourth root of the fermion determinant. The partition function reads:

$$Z \equiv \int \mathcal{D}U e^{-S_G} \det D^{\frac{1}{4}}[U, q_u] \det D^{\frac{1}{4}}[U, q_d] \quad (9)$$

$$D_{i,j}^{(q)} \equiv am\delta_{i,j} + \frac{1}{2} \sum_{\nu=1}^4 \eta_\nu(i) \left(u_\nu^{(q)}(i) U_\nu(i) \delta_{i,j-\hat{\nu}} - u_\nu^{*(q)}(i-\hat{\nu}) U_\nu^\dagger(i-\hat{\nu}) \delta_{i,j+\hat{\nu}} \right) \quad (10)$$

$\mathcal{D}U$ is the integration over $SU(3)$ gauge link variables, S_G is the plaquette action, i, j are lattice site indexes, $\eta_\nu(i)$ are the staggered phases. The quark charges are $q_u = 2|e|/3$ and $q_d = -|e|/3$. The density of the integrand in Eq. (4) can be expressed as

$$M \equiv a^4 \frac{\partial f}{\partial b} = \frac{1}{4L_t L_s^3} \sum_{q=u,d} \left\langle \text{Tr} \left\{ \frac{\partial D^{(q)}}{\partial b} D^{(q)-1} \right\} \right\rangle \quad (11)$$

where L_s and L_t are the temporal and spatial sizes ($T = 1/(L_t a)$). Let us stress again that M is not the magnetization of the system, but just the derivative of the interpolation of the free energy between integer quanta, which has no direct physical interpretation.

We have explored different lattice spacings and pseudo-Goldstone pion masses, by tuning the inverse gauge coupling β and am according to Ref. [19] (the magnetic background does not modify a [17, 20]), and different values of L_s and L_t (see Table I). We have adopted a Rational Hybrid Monte-Carlo (RHMC) algorithm implemented on GPU cards [21], with statistics of $O(10^3)$ molecular dynamics (MD) time units for each value of b . The observable in Eq. (11) has been measured every 5 trajectories,

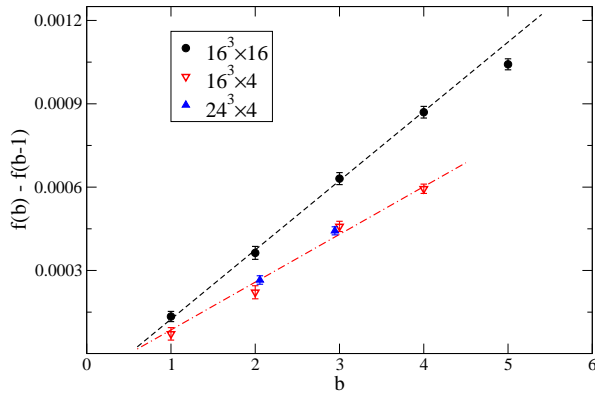


FIG. 2: $f(b) - f(b-1)$ computed from the data reported in Fig. 1, together with best fits obtained, for $b \leq 4$, according to $c_2(2b-1)$ (see Eq. (12)). Two further, properly rescaled data points are reported from a $24^3 \times 4$ lattice.

of one MD time unit each, adopting a noisy estimator, with 10 random vectors for each measure.

Fig. 1 shows an example of the determination of M , for the first 4 quanta of B , for one parameter set and two different temporal sizes, $L_t = 4$ and 16, the latter being taken as our $T \sim 0$ reference value. Oscillations between successive quanta can be related to the presence of the string: a couple of harmonics are visible, associable with the d and u quark contributions, which feel the string differently.

Despite the unphysical oscillations, M is smooth enough to perform a numerical integration: that is done by using a spline interpolation over 16 equally spaced determinations of M for each quantum; errors are estimated by means of a bootstrap analysis. We have checked that variations due to different integration schemes, or to different interpolating strategies and densities, always stay well within the estimated errors, so that the integration procedure is in fact very robust (see Appendix A for details).

To obtain the $\mathcal{O}(B^2)$ term in $\Delta f_R(B, T)$, we have determined the $\mathcal{O}(B^2)$ contributions to both $\Delta f(B, T)$ and $\Delta f(B, 0)$, then we have subtracted them; consistent results are obtained if the subtraction is performed first. Assuming that $a^4 \Delta f(b) \equiv c_2 b^2 + \mathcal{O}(b^4)$ holds for integer b , c_2 is conveniently determined by looking at the differences between successive quanta,

$$a^4 (f(b) - f(b-1)) \equiv \int_{b-1}^b M(\tilde{b}) d\tilde{b} \simeq c_2 (2b-1). \quad (12)$$

In this way, one does not need to determine the whole difference $f(b) - f(0)$, and fitted data have independent errors, since the integration uncertainties do not propagate between consecutive quanta.

The finite differences obtained from the data in Fig. 1 are reported in Fig. 2. A fit to $c_2(2b-1)$ works well for $b \leq 4$, yielding $c_2 = 0.861(20) \times 10^{-4}$ ($\chi^2/\text{d.o.f.} = 5.4/3$) for $L_t = 4$ and $c_2 = 1.309(21) \times 10^{-4}$ ($\chi^2/\text{d.o.f.} = 0.5/3$)

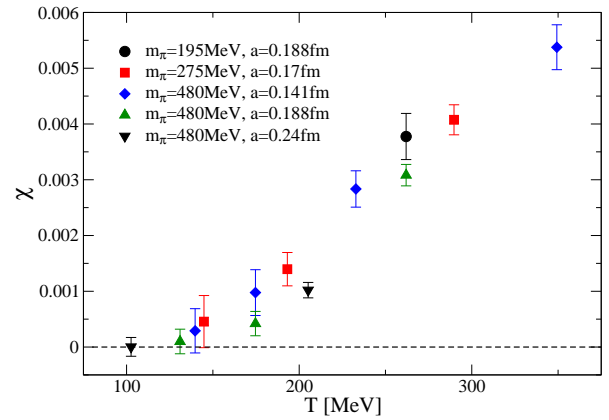


FIG. 3: Susceptibility $\chi = \tilde{\chi}/(1 - \tilde{\chi})$ (SI units) as a function of T , for different values of m_π and a .

for $L_t = 16$. Two further data points are reported from a $24^3 \times 4$ lattice, after proper rescaling, to check for spatial volume independence. Finally, we get $a^4 \Delta f_R = c_2 b^2 + \mathcal{O}(b^4)$, with $c_{2R} = -0.448(29) \times 10^{-4}$. The agreement with a quadratic behavior confirms that the medium has a linear response, at least for small fields, and excludes different possibilities, e.g., ferromagnetic-like.

The determination of $\tilde{\chi}$ from Eq. (8) requires a conversion into physical units for Δf_R and b , according to Eq. (2). The result is

$$\tilde{\chi} = -\frac{2|e|^2 \mu_0 c}{18 \hbar \pi^2} L_s^4 c_{2R}, \quad (13)$$

where the constants \hbar and c have been reintroduced explicitly, in order to permit a conversion to SI units. We obtain $\tilde{\chi} = 0.00306(19)$, i.e. a paramagnetic behavior. The same procedure, described in detail for one case, has been repeated for the various combinations of m_π , T and a reported in Table I, obtaining the results reported in Table I and in Fig. 3.

IV. DISCUSSION

Fig. 3 shows that χ is nearly zero in the confined phase, while it rises roughly linearly with T in the deconfined one. The obtained values, when compared with those of ordinary materials¹, indicate strong paramagnetism. The drastic increase of χ , which is naturally associable to quark liberation, implies a proportional increase of the B -dependent (quadratic) contribution to the pressure.

At $m_\pi \simeq 480$ MeV, we performed a continuum extrapolation according to: $\chi = A(T - \tilde{T}) + A' a^2$, which turns out to be an effective description of all data with $T > 170$ MeV ($\chi^2/\text{d.o.f.} = 2.5/3$), with coefficients

¹ Most paramagnetic metals have χ in the range $10^{-5} - 10^{-4}$

$A = 2.73(24) \times 10^{-5} \text{ MeV}^{-1}$, $A' = -7.6(3) \times 10^{-4} \text{ GeV}^2$ and $\bar{T} = 126(16) \text{ MeV}$. When m_π decreases, only a very slight increase of χ can be observed.

The computation proposed and first performed in this study surely claims for an extension to the physical case. Our results do not suggest drastic changes when decreasing the pion mass. However, the inclusion of the strange quark may change results quantitatively. If one tries to separate the contributions to χ from u and d quarks, see Eq. (11), one obtains roughly $\chi_u \sim 4\chi_d$, as expected naively on a charge counting basis (see Appendix A for details). Therefore we expect that including the strange quark may increase χ by about 20 %. An extension to the case of chromomagnetic fields may be interesting as well [22].

Finally, we notice, following Ref. [23], that the strong paramagnetic behavior, rising with T , in the deconfined phase, and the fact that finite a effects tend to diminish it, may explain the lowering of the pseudocritical temperature with B [17], and why a different behavior was observed on coarse lattices [24, 25].

Acknowledgments

We thank E. D'Emilio, E. Fraga and S. Mukherjee for useful discussions. Numerical computations have been performed on computer facilities provided by INFN, in particular on two GPU farms in Pisa and Genoa and on the QUONG GPU cluster in Rome.

Appendix A

We discuss in this section a few additional results from our simulations, in order to better elucidate some details of our procedure and to check for possible systematic effects.

The first question one could ask regards the stability of the results against a change of the integration procedure, adopted to exploit Eq. (4). To that purpose, we report in Table II the results of the integration over one given quantum of field (reference parameters are the same as for Fig. 1), obtained by varying the order of the spline interpolation used by the integrator and/or the number of points over which M is evaluated. It turns out that the integration is extremely stable, with variations well below statistical fluctuations.

A different issue regards the stability of the result of Eq. (4) against a variation of the free energy interpolation. The simplest, alternative interpolation, consists in allowing for two (or more) different Dirac strings at the same time, located in different points. That is achieved by superposing two $U(1)$ fields like that in Eq. (3), but with one of them shifted in one or two coordinates, so as to move the location of the string: in this way one obtains an interpolation between two consecutive, even quanta, however odd quanta are not possible any more. In Fig. 4

s	16 points	32 points
1	0.001192(32)	0.001187(25)
2	0.001188(35)	0.001186(25)
3	0.001184(35)	0.001188(25)
4	0.001183(34)	0.001188(27)

TABLE II: Result of the integration of M between $b = 3$ and $b = 4$ on a $16^3 \times 4$ lattice (with $m_\pi \approx 480 \text{ MeV}$ and $a \approx 0.188 \text{ fm}$) using different methods: s is the degree of the spline interpolation and the integral is computed starting from meshes of 16 or 32 equally spaced points.

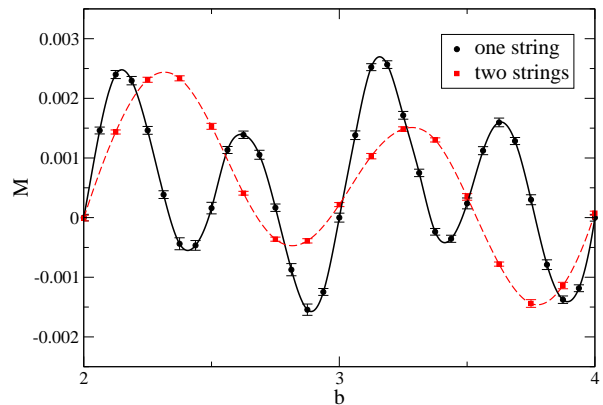


FIG. 4: M computed between $b = 2$ and $b = 4$, and for the same lattice parameters as in Table II, for two different interpolations of the free energy (see text).

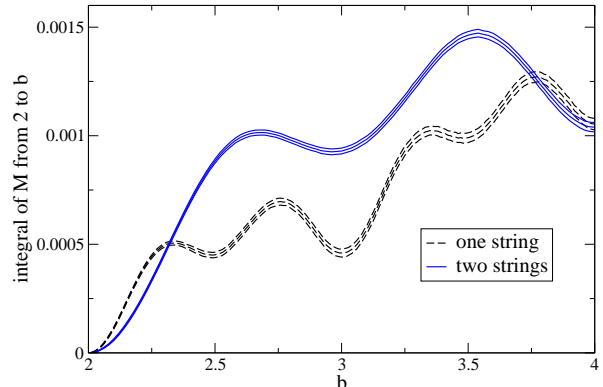


FIG. 5: Cumulative integrals of the two functions reported in Fig. 4.

we show, as an example, the values of M between $b = 2$ and $b = 4$ obtained for the standard and for the alternative interpolation described above: in the latter case, the two Dirac strings pierce the x, y plaquettes located at $(n_x, n_y) = (L_x, L_y)$ and $(L_x, L_y/2)$, respectively. The corresponding cumulative integrals are reported in Fig. 5: they coincide, within errors, for values of b where strings become invisible for both interpolations, proving the stability of the procedure.

Finally, since the observable M is made up of two dif-

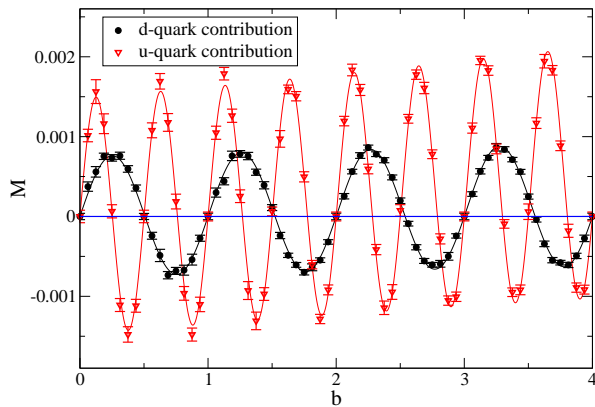


FIG. 6: Contributions to M from the u and d quarks, computed on a $16^3 \times 4$ lattice, with $a \approx 0.188$ fm and $m_\pi \approx 480$ MeV. The continuous lines are best fits according to Eq. (A1).

ferent terms, M_u and M_d , coming from each quark determinant (see Eq. (11)), it is interesting to see how the two contributions look like. That is shown in Fig. 6, where the same data shown in Fig. 1 for the $16^3 \times 4$ lattice have been split accordingly. M_u and M_d present very similar oscillations, apart from a factor two in the frequency, which can be trivially associated to the electric charge ratio of the two quarks. It is interesting that results can be described by the simplest function which can be devised by requiring that: *i*) it vanishes at points where

the string becomes invisible to the corresponding quark; *ii*) it has a non-vanishing integral between any consecutive pair of such points; *iii*) it is an odd function of b , as required by the charge conjugation symmetry present at $b = 0$. Such function is

$$M_q^{\text{try}} = A \sin\left(2\pi \frac{q}{q_d} b\right) + A' b \left(1 - \cos\left(2\pi \frac{q}{q_d} b\right)\right) \quad (\text{A1})$$

where $q = q_u$ or $q = q_d$, and fits very well all data in Fig. 6, with $\chi^2/\text{d.o.f.} = 0.81$ for the d quark and $\chi^2/\text{d.o.f.} = 1.10$ for the u quark. It is easy to check that the integral of such function between 0 and integer values of b equals $A' b^2/2$ (fit values for A' are compatible with those from the standard spline integrators), therefore deviations from such simple description are expected as soon as the corrections to the quadratic behavior of Δf become visible.

Data obtained for M_u and M_d can be integrated separately for each lattice setup, in this way also the renormalized free energy and the corresponding magnetic susceptibility can be separated into two different contributions, $\chi = \chi_u + \chi_d$. For the case shown explicitly in Fig. 6, one obtains $\chi_u = 2.43(18)$ and $\chi_d = 0.63(6)$. Even if one cannot strictly speak of u and d contributions, because of quark loop effects which mix the two terms, it is nice to observe that $\chi_u/\chi_d = 3.9(4) \sim (q_u/q_d)^2$, in agreement with a naive charge counting rule. Similar results are obtained for the other values of T and m_π explored in this study.

-
- [1] T. Vachaspati, Phys. Lett. B **265**, 258 (1991).
 - [2] D. Grasso and H. R. Rubinstein, Phys. Rept. **348**, 163 (2001) [astro-ph/0009061].
 - [3] V. Skokov, A. Y. Illarionov and V. Toneev, Int. J. Mod. Phys. A **24**, 5925 (2009) [arXiv:0907.1396 [nucl-th]].
 - [4] V. Voronyuk, V. D. Toneev, W. Cassing, E. L. Bratkovskaya, V. P. Konchakovski and S. A. Voloshin, Phys. Rev. C **83**, 054911 (2011) [arXiv:1103.4239 [nucl-t]].
 - [5] A. Bzdak and V. Skokov, Phys. Lett. B **710**, 171 (2012) [arXiv:1111.1949 [hep-ph]].
 - [6] W. -T. Deng and X. -G. Huang, Phys. Rev. C **85**, 044907 (2012) [arXiv:1201.5108 [nucl-th]].
 - [7] R. C. Duncan and C. Thompson, Astrophys. J. **392**, L9 (1992).
 - [8] D. Kharzeev, K. Landsteiner, A. Schmitt and H. -U. Yee, Lect. Notes Phys. **871**, 1 (2013).
 - [9] P. V. Buividovich, M. N. Chernodub, E. V. Luschevskaya and M. I. Polikarpov, Nucl. Phys. B **826**, 313 (2010) [arXiv:0906.0488 [hep-lat]].
 - [10] G. S. Bali, F. Bruckmann, M. Constantinou, M. Costa, G. Endrodi, S. D. Katz, H. Panagopoulos and A. Schafer, Phys. Rev. D **86**, 094512 (2012) [arXiv:1209.6015 [hep-lat]].
 - [11] G. S. Bali, F. Bruckmann, G. Endrodi, F. Gruber and A. Schaefer, JHEP **1304**, 130 (2013) [arXiv:1303.1328 [hep-lat]].
 - [12] G. 't Hooft, Nucl. Phys. B **153**, 141 (1979).
 - [13] J. Smit and J. C. Vink, Nucl. Phys. B **286**, 485 (1987).
 - [14] P. H. Damgaard and U. M. Heller, Nucl. Phys. B **309**, 625 (1988).
 - [15] M. H. Al-Hashimi and U. J. Wiese, Ann. Phys. **324**, 343 (2009) [arXiv:0807.0630 [quant-ph]].
 - [16] P. de Forcrand, M. D'Elia and M. Pepe, Phys. Rev. Lett. **86**, 1438 (2001) [hep-lat/0007034].
 - [17] G. S. Bali, F. Bruckmann, G. Endrodi, Z. Fodor, S. D. Katz, S. Krieg, A. Schafer and K. K. Szabo, JHEP **1202**, 044 (2012) [arXiv:1111.4956 [hep-lat]].
 - [18] L. D. Landau, E. M. Lifshitz and L. P. Pitaevskii "Electrodynamics of continuous media" Butterworth-Heinemann (2004).
 - [19] T. Blum, L. Karkkainen, D. Toussaint and S. A. Gottlieb, Phys. Rev. D **51**, 5153 (1995) [hep-lat/9410014].
 - [20] M. D'Elia, M. Mariti and F. Negro, Phys. Rev. Lett. **110**, 082002 (2013) [arXiv:1209.0722 [hep-lat]].
 - [21] C. Bonati, G. Cossu, M. D'Elia and P. Incardona, Comp. Phys. Comm. **183**, 853 (2012) [arXiv:1106.5673 [hep-lat]].
 - [22] P. Cea and L. Cosmai, JHEP **0508**, 079 (2005); P. Cea, L. Cosmai and M. D'Elia, JHEP **0712**, 097 (2007);
 - [23] E. S. Fraga, J. Noronha and L. F. Palhares, arXiv:1207.7094 [hep-ph].
 - [24] M. D'Elia, S. Mukherjee, F. Sanfilippo, Phys. Rev. D **82**, 051501 (2010).

- [25] E. -M. Ilgenfritz, M. Kalinowski, M. Muller-Preussker, B. Petersson and A. Schreiber, Phys. Rev. D **85**, 114504 (2012).